Coverage Improvement of Aeronautical Communication Services based in the Azores

Beatriz Ferreira
Portuguese Air Force Academy[i]/ Instituto Superior Técnico[ii]
Portuguese Air Force[i]/ University of Lisbon[ii]
Sintra[i]/ Lisbon[ii], Portugal
biferreira@academiafa.edu.pt

Luís M. Correia
Instituto Superior Técnico / INOV-INESC
University of Lisbon
Lisbon, Portugal
luis.m.correia@tecnico.ulisboa.pt

Anna Agamyrzyansc
Portuguese Air Force / Lisbon, Portugal
anna@emfa.pt

***Abstract*— The purpose of this dissertation is to investigate the theoretical concepts required to solve the coverage problem verified in the military aeronautical communications system that will be implemented in the Azores Archipelago. The majority of the concepts investigated are related to the perception of the coverage problem. The characteristics of the communication system that was once installed in the Azores are presented in the dissertation, theoretical concepts on coverage as well as propagation models are studied, and a state of the art on the subject is presented. Following that, the model is developed, its analysis is performed, and the results obtained are evaluated. Finally, the results of this research conducted throughout the dissertation will be presented.**

Keywords-component; Coverage; Aeronautical Military Communications; VHF-AM Communication System.

I. INTRODUCTION

The Portuguese Air Force (FAP) performs several missions in the Azores Archipelago, therefore there is a need to install an aeronautical communication and navigation system in it.

The sovereignty of a State depends on the rights and freedoms that are guaranteed to its citizens. The Armed Forces (FA) assist in the task of ensuring the security of Portuguese citizens. This is due to the fact that FAs are entrusted with population support and civil protection missions [1].

The FAP, as an integral part of the national forces system, has the mission to cooperate in the defence of the military and the Republic. Thus, it is responsible for carrying out air operations in defence of national space as well as missions of public interest to meet the needs of populations [2]. As the Portuguese territory is made up of Mainland Portugal and the Autonomous Regions of the Azores and Madeira, it is necessary to guarantee the safety and satisfaction of the needs of everyone who inhabits these regions.

Air Base nº4 (BA4) - Lajes Air Base has been part of the the Command of the Azores' Aerial Zone (CAA) since 1978. Since then, it has been assigned several missions, including Search and Rescue (SAR), Tactical Transport, and Maritime Patrol in the Archipelago Area. However, currently, BA4 not only maintains these missions but also provides support to local populations and civil authorities, namely in carrying out sanitary evacuations and inter-island transport [3]. The execution of these missions is carried out in the Flight Information Region (FIR).

For the execution of this mission, there are two detached aircraft at Lajes Air Base that carry out the three types of mission mentioned above. The aircraft in question is the EADS C-295M fixed-wing aircraft, with a maximum range of 770 nm, 1,426 km, and a maximum range of 10 h, and the AUGUSTA-WESTLAND EH-101 MERLIN helicopter, with a maximum range of 400 nm, 740 km, and a maximum range of 8h30, when considering the typology of SAR missions [4] [5].

The SAR area under the responsibility of CAA is a large area and, as such, it is necessary to have means of communication between the ground stations and the aircraft so that they can efficiently carry out their mission. Since, for the most part, the missions carried out by the aircraft are SAR and medical evacuation missions, it is necessary that the means of communication and navigation support allow these missions to be carried out as quickly as possible. However, the system that was installed in the Azores had a coverage area much smaller than the area that the aircraft can reach and still presented several shaded areas. In order to better understand the importance of this airbase and the communications system based on it, the number of missions carried out by the aforementioned aircraft, associated with the respective mission, and the number of associated flight hours were surveyed.

In 2020, only in the Azores Archipelago, 365 patient air transport missions were accounted for, resulting in a total of 457 transported patients and 1,068 flight hours. A total of 31 rescue missions on ships were also counted, resulting in a total of 29 patients rescued throughout the FIR, totalling 201 hours of flight for this mission, 39 SAR missions were also counted which resulted in 6 rescues, totalling 201 hours of flight. There were also 30 missions carried out, which resulted in a total of 76 hours of air transport of organs [6].

II. STATE OF THE ART

The military communications system, currently inoperative, headquartered in the Azores operated in the VHF range and was intended to facilitate communications between the SAR aircraft and the core of the BA4 operations. [7].

In the communications between the different sites, the signals were modulated in frequency (FM – Frequency Modulation) and, to establish these connections, directional antennas were used [7].

Regarding ground-to-air and air-to-ground communications, the signals were amplitude modulated (Amplitude Modulation - AM). Communications between the aircraft and the sites were established at the nominal frequency of 139.3 MHz. The system to be installed will use the same nominal frequency, however, it will use it with a difference of 5 kHz between transmitters. Each ground station transmits a

signal within a 25 kHz bandwidth with a specific offset associated with each ground station [7].

With the restructuring of the communications system, it is intended that it mainly ensure low-altitude communications using the sites on Terceira island, São Miguel island, Faial island, Flores island, and a new site installed on the island. Santa Maria. Concerning the minimum radius, it is intended that this is 200 km and a minimum altitude of 600 m, maintaining the operational requirements for the system previously [8]. Thus, it is intended to improve the coverage area of the VHF communications system to help in the SAR operations to be carried out at the FIR, which is under the responsibility of the CAA.

With the increase of air traffic in oceanic areas the need to communicate at distances beyond the horizon radio distance became a problem to be solved, as such, VHF systems became a possibility to overcome this problem. This is since signals can propagate in various ways, for example, by atmospheric refraction or diffraction. However, all types of propagation of this type of signals will lead to high attenuation levels that can be exceeded if systems such as high-power amplifiers in transmitters, low-noise pre-amplifiers in receivers, or high-gain antennas are considered [9]. In the problem under study in this dissertation, omnidirectional and sectorial antennas will be analyzed due to the type of communication under study.

About 20 over-the-horizon VHF systems have been deployed by Park Air Systems, these have been deployed in places such as Greenland, Iceland, and China. Currently, the company chooses to propose improved solutions for this system, solutions presented in [10]. The systems under review were built and tested in the UK and later transported and installed in the locations where they were to operate [11].

The system implemented in China has exceeded expectations in that it provides long-range air traffic communications along the South China Sea [11]. In this system, the transmitter is connected to a pair of directional antennas aligned to project a beam in the necessary direction. Each antenna is composed of a six-element Yagi array with dipole-type radiators, each dipole mounted on horizontal support where, later, they are mounted on a tower with a power level of 750 W. The horizontal width of the resulting beam is 90º and the vertical width is 60° [11].

Another success story regarding the increase in the coverage area of the VHF system is the increase in coverage of Indian airspace over the ocean, presented in the ICAO report. The coverage of the Mumbai and Trivandrum airport air control center was optimized with the installation of a Remote-Controlled Air to Ground Communication (RCAG) Communications System on the island of Agatti. To allow for improvements in addition to those already implemented, the Airports Authority of India (AAI) installed a high-power VHF transmitter with a directional antenna in Chennai and Port Blair and a high-power transmitter in Calcutta and Visakhapatnam [12].

III. Model Development and Implementation

A. Aeronautical communications system under study

The military communications system, which is no longer operational and is based in the Azores, operated in the VHF band and was designed to facilitate communications between SAR aircraft and the BA4 operations core [7].

The system included two types of communications: ground-to-air communications (VHF-AM), which were the subject of this dissertation, and ground-to-ground communications (VHF-FM).

The nominal frequency of 139.3 MHz was used for communications between aircraft and ground stations. The system to be installed will use the same nominal frequency, but with a 5 kHz difference between transmitters. As a result, each ground station transmits a signal with a specific offset within a bandwidth of 25 kHz [7].

When considering the communications system that will be restructured in this dissertation, which is currently inactive, the goal was to ensure a signal greater than 4 μV in a radius of 110 nm, equivalent to 200 km, at an altitude of at least 2 000 feet, equivalent to 600 m [7].

The restructuring of the communications system is intended to primarily ensure low-altitude communications by utilizing the terrestrial stations of Terceira, São Miguel, Faial, and Flores islands, as well as a new ground station installed on the island of Santa Maria. The operational requirements for the minimum radius and minimum altitude remain the same as for the previously installed system [13].

Table 1 shows the exact locations of the ground stations of the new communications system to be installed in the Azores Archipelago.

Table 1.The location of the new communications system's ground stations (taken from [13]).

Base Station	**Flores**	**Faial**	**Terceira**	**São Miguel**	**Santa Maria**
Local	Morro Alto	Cabelo Gordo	Santa Bárbara	Barrosa	Pico Alto
Latitude [N]	39º27’ 48’’	38º34’ 33’’	38º43’47’’	37º45’3 5’’	36º58’5 9’’
Longitude [W]	31º13’ 13’’	28º42’ 47’’	27º19’06’’	25º29’3 1’’	25º05’2 7’’
Altitude [m]	979	1108	1015	972	561

B. Application Scenario

Two different aircraft are considered in the problem being solved, and as a result, they serve different purposes in carrying out SAR missions. The fixed-wing aircraft, C-295M, aids in the realization of the SAR mission by launching a life raft into the sea, while the mobile wing aircraft, EH-101 Merlin, can collect people [14].

The maximum range of the fixed-wing aircraft is 1 420 km. Because of its greater range, this aircraft can detect and assist targets subject to search and rescue at greater distances [14]. The ability of the mobile wing aircraft to remain immobile and relatively stable on the target subject to the SAR mission allows it to carry out rescues. It does, however, have a 740 km radius of action [14].

These missions can be carried out at various altitudes by aircraft. Several scenarios should be considered for this, each of which can be defined by one or more altitudes attained by the aircraft.

Figure 1 depicts the most common altitudes attained by the two aircraft while carrying out this type of mission [13].

Table 2 summarizes the communication system requirements to be considered for development.

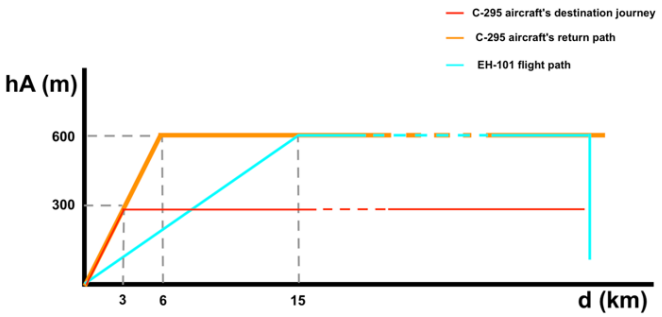

Figure 1. The flight paths of the C-295M and EH-101 Merlin aircraft.

Table 2. A summary of the requirements for the communications system.

Connection Frequency [MHz]	139.3	
Minimum coverage altitude [m]	20	
Maximum coverage altitude [m]	600	
Minimum coverage radius [km]	200	
Altitude of earth station antennas [m]	Flores	999
	Faial	1128
	Terceira	1035
	São Miguel	992
	Santa Maria	581

C. *Model description*

The developed model, whose block diagram is shown in Figure 2, aims to maximize system coverage while minimizing shadow areas as much as possible.

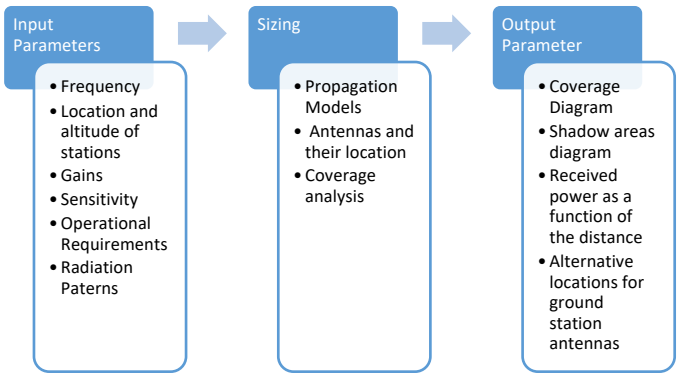

Figure 2. A high-level overview of the model to be implemented

The propagation models that could be applied to the model to be developed were analysed in order to understand if they would have applicability and what the minimum and maximum distances of application of each of the models are for the correct dimensioning of the problem under study. These calculations are necessary in order to calculate the path losses. The path losses value will be required to calculate the received power as a function of distance, which will be compared to the sensitivity values to perceive the system's coverage and shadow areas. As a result, the received power is expressed through

$$P_{r_{[\mathrm{dBm}]}} = P_{t_{[\mathrm{dBm}]}} + G_{t_{[\mathrm{dBi}]}} + G_{r_{[\mathrm{dBi}]}} - L_{p_{[\mathrm{dB}]}} \quad (1)$$

where:

- P_t: emission power;
- G_t: gain of the transmit antenna;
- G_r: gain of the receiver antenna;
- L_p: path losses.

The operating requirements to be considered are shown in Table 3. Taking them into consideration, the presented reception power was reduced to its bare minimum.

Table 3. Operating requirements based on the system's characteristics

Antenna	$G_{r_{[dBi]}}$	$f_{[MHz]}$	$P_{r_{min[dBm]}}$	$P_{t_{[dBm]}}$
EH-101	-3	139.3	-95	43
C-295M				
Ground Station	4.65			

We started by looking at the equations that define the simplest propagation situation, which is when the aircraft is in line of sight (LOS) with the ground station antenna. As a result, this model is applicable in situations where the aircraft is close to the ground station, such as near an airport. As a result, the only existing attenuation factor for LOS connections is the free space attenuation, which is given by

$$L_{0[\mathrm{dB}]} = 32.44 + 20\log_{10}(d_{[\mathrm{km}]}) + 20\log_{10}(f_{[\mathrm{MHz}]}) \quad (2)$$

where:

- d : distance between the terminals.

The deduced expression (3) was used to evaluate the maximum distance of application of the current model.

$$d_{maxEL[m]} = \frac{w_{[m]}^2 \lambda}{r_{e\,[m]}^2 - w_{[m]}\lambda} \quad (3)$$

where:

- r_e : radius of the first Fresnel ellipsoid at distance w from the first terminal;
- w : distance from the first terminal to the point where the ellipsoid radius is calculated.

The possibility of employing the flat earth model was then considered. When communications are carried out over short distances, in the order of tens of kilometers, the Earth is modeled as a flat surface in the model under consideration. To assess the model's applicability, the minimum and maximum distances for applying the model were calculated. When the model's minimum and maximum applicability distances are compared, it is determined that this model is not suitable for use in the model. This is due to the fact that the minimum applicability distance exceeds the maximum distance. As a result, the application of the model's flat earth propagation model is excluded.

Then, the possibility of employing the Spheric Earth Model had to be assessed.

However, it is necessary to assess whether the diffraction phenomenon is prevalent; if the diffraction phenomenon prevails, the losses are given by the trans-horizon communication model, which will be presented in the future. Thus, the limit angle of incidence [15] is a value to consider when understanding the possibility of using this equivalence.

The curvature of the Earth also interferes with the range of the connection when considering the maximum distance of

application of the model; thus, the Radio Horizon distance is considered as the maximum distance that it is possible to maintain the connection in LOS; this situation is depicted in Figure 3.

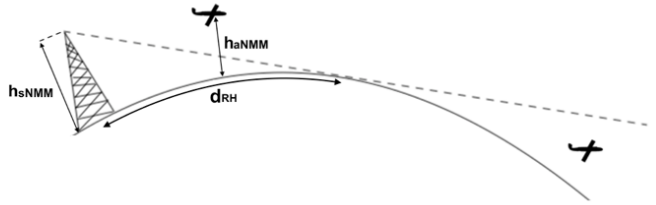

Figure 3. Exemplary scheme of the influence of the radio horizon distance.

Expression (3) gives the maximum distance at which the aircraft can communicate in LOS with the nearest ground station.

When the minimum distance of application of the Spherical Earth Model is compared to the maximum distance of application of the current model, it is concluded that the Spherical Earth Model has no applicability in the problem under consideration. This is because, for all cases under consideration, the maximum distance of application of the model is less than the minimum distance of application of the same when the incidence angles are taken into account.

Diffraction across the Earth's surface is a permanent propagation mechanism for frequencies above 30 MHz reaching distances beyond the horizon. Because the connection to be considered in the communication system under study uses a frequency of 139.3 MHz, this mechanism should be considered. However, while diffraction can reach beyond the horizon, it can also interfere with the system and cause losses [16].

The total loss due to diffraction [16] in a connection with distance, d

$$L_{p_{[\mathrm{dB}]}} = L_{0_{[\mathrm{dB}]}} - [F(X) + G(Y_1) + G(Y_2)\,] \tag{4}$$

This model will be used to validate the existence of over-horizon communications. Because neither the Flat Earth nor the Spherical Earth models can be used in this case, the minimum application distance of this model is equal to the maximum application distance of the Free Space propagation model.

It is also necessary to consider the potential major obstacles to the connection. Losses due to diffraction in obstacles must also be considered if the connection is not unobstructed. As a result, the degree of impairment of the first Fresnel ellipsoid must be investigated. The greater the attenuation caused by the first obstructed Fresnel Ellipsoid, the greater the value of v, the degree of obstruction of the connection, given by equation (5) [16].

$$v = h_{OEF[\mathrm{m}]}\sqrt{\frac{2\ d_{[\mathrm{m}]}}{\lambda_{[\mathrm{m}]}\ d_{T_xO[\mathrm{m}]}\ d_{OR_x[\mathrm{m}]}}} \tag{5}$$

where:

- h_{OEF}: difference between the height of the obstacle's top and the center of the Fresnel Ellipsoid (can be negative if the obstacle is lower than the center of the ellipsoid);
- d_{T_xO} : the distance between the transmitter and the obstacle;
- d_{OR_x}: the distance between the obstacle and the receiver.

The obstacle attenuation can be calculated using the degree of obstruction of the ellipsoid. The Knife-Edge model's obstacle attenuation for v greater than - 0.7 is given by (6). Attenuation can be ignored if the value of v is less than -0.7 [16].

$$L_{KE[\mathrm{dB}]} = 6.9 + 20\log_{10}(\sqrt{(v-0.1)^2+1} + v - 0.1) \tag{6}$$

As a result, this model will be used whenever there are obstacles in the path of the connection. If there is only one obstacle, the Knife-Edge Model will be applied directly. If there are multiple obstacles obstructing the connection, the Deygout model will be used, multiplying the application of the Knife-Edge model to several segments of the path between the terminals and adding the different values of the obstacle attenuation.

Thus, after considering the models presented above, it was determined that the model to be developed should adhere to the generic considerations presented in Figure 4. in order to solve the problem under study.

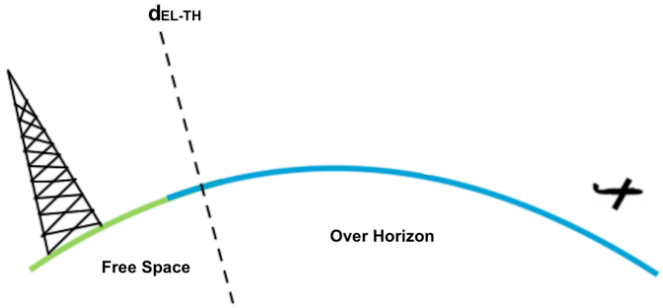

Figure 4. The model's development guidelines.

Fading is a factor that frequently affects the performance of wireless communication channels. The two most common types of fading should be considered for the communications under study: slow fading and fast fading. Because there is always movement in one of the terminals in the case under consideration, the system will always be subject to fast fading [18].

According to [19], the scenario to be considered for the problem under consideration is one in which the aircraft is in motion. As a result, the Rice distribution is the appropriate statistical distribution to define this type of fading. Thus, for the case where the aircraft is in motion, a typical value for the Rice constant is K=15 dB.

The gain of the antennas is another factor that will influence the results. This isn't a fixed number. The radiation diagram of the emitting and receiving antennas determines this. Thus, the gain of the antennas as a function of the terminal position relationship is given by (7).

$$G(\phi,\theta)_{A/E[dBi]} = G_{maxA_{[dBi]}} + 10\log_{10}(f_{A\backslash E}(\theta)) + 10\log_{10}(f_{A\backslash E}(\phi)) \tag{7}$$

where:

- $G(\theta,\phi)_{A\backslash E}$: a rough estimate of the antenna gain of the aircraft/ground station;
- $G_{maxA\backslash E}$: maximum antenna gain of an aircraft/ground station;
- $f_{A\backslash E}(\theta)$: normalized radiation diagram of the

aircraft/ground station antenna in the vertical plane;

- $f_{A\backslash E}(\phi)$: normalized radiation diagram of the aircraft/ground station antenna in the horizontal plane.

The antennas installed in the aircraft are monopoles of a tenth of a wavelength, as the wavelength and radiation diagrams are given by (8) and (9).

$$f_A(\theta) = \begin{cases} (\sin\theta)^2, & \theta_{min} < \theta \leq 90º \\ 0.001, & 0 \leq \theta \leq \theta_{min} \\ \theta_{min} = 1{,}81º \end{cases} \quad (8)$$

$$f_A(\phi) = \begin{cases} 1, & 330º \leq \phi \leq 30º \wedge 60º \leq \phi \leq 300º \\ 0.5, & 300º \leq \phi \leq 330º \wedge 30º \leq \phi \leq 60º \end{cases} \quad (9)$$

In terms of earth station antennas, tests will be performed using omnidirectional and sectorial antennas to determine which ones will be best suited to the system. As a result, two omnidirectional antennas with varying gain values and a sectorial antenna will be considered.

The vertical and horizontal radiation diagrams of an omnidirectional antenna with a maximum gain of 2.2 dBi are described by (10) and (11), respectively.

$$f_{ET}(\theta) = \left| \frac{\cos\left[\frac{\pi}{2}\cos(\theta)\right] - \cos(\frac{\pi}{2})}{\sin(\theta)} \right|^2 \quad (10)$$

$$f_{ET}(\phi) = 1 \quad (11)$$

The second omnidirectional antenna has a maximum gain of 5.2 dBi and is represented by vertical and horizontal radiation diagrams (12) and (11), respectively.

$$f_{ET}(\theta) = \left| \frac{\cos\left[\frac{\pi}{2}\cos(\theta)\right] - \cos(\frac{\pi}{2})}{\sin(\theta)} \right|^2 \frac{1}{3}\frac{\sin(3\,\pi\,\cos(\theta))}{\sin(\pi\cos(\theta))} \quad (12)$$

If these antennas are not installed on the support towers, their horizontal diagram will change, and the horizontal radiation diagram will be described by (13).

$$f_{ET}(\phi) = \frac{1-\cos(\phi)}{2} \quad (13)$$

After that, the sectorial antenna was examined. This antenna has a maximum gain of 7.2 dBi, and its vertical and horizontal radiation diagrams are described by expressions (14) and (15), respectively.

$$f_{ET}(\theta) = \left| \frac{\cos\left[\frac{\pi}{2}\cos(\theta)\right] - \cos(\frac{\pi}{2})}{\sin(\theta)} \right|^2 \frac{1}{3}\frac{\sin(3\,\frac{5\pi}{2}\cos(\theta))}{\sin(\frac{5\pi}{2}\cos(\theta))} \quad (14)$$

$$f_{ET}(\phi) = \frac{1+\frac{\cos(\phi)}{2}}{1.5} \quad (15)$$

D. Model Assessment

The values shown in Table 3 and the altitude of the terrestrial station, which is located on the island of Santa Maria, will be used to carry out the tests. As a result, for the described tests, an elevation profile associated with the same terrestrial station will be used, the profile that corresponds to 240º using the North Pole as a reference point, that is, 0º.

As a result, we began by determining whether the path losses for the Free Space Model and the Trans-Horizon Model vary with distance as expected. For both models, the received power was evaluated as a function of distance. Following a comparison of the model's results, these were crossed with calculations performed manually. The crossing of the obtained results revealed that the results were in line with what was expected.

The path losses of the over-horizon model were then examined while the aircraft's flight altitudes were taken into account. Based on the results of the tests, it was discovered that for flight altitudes below 6565 m, this has no effect on the model's evolution. Thus, the curves of received power as a function of distance are superimposed for the three flight altitudes under consideration.

The next test evaluated the developed model's evolution of received power as a function of distance. Because the developed model employs two distinct propagation models, a transition zone between the two is to be expected. This transition zone, similar to a step, is determined by the terminal altitude, so it occurs at different distances for the three flight altitudes.

As shown in Figure 5, the results are as expected. That is, when the Free Space propagation model is used, there are three overlapping curves up to the respective transition distance between models, and then there is a new overlap when the over-horizon model is used.

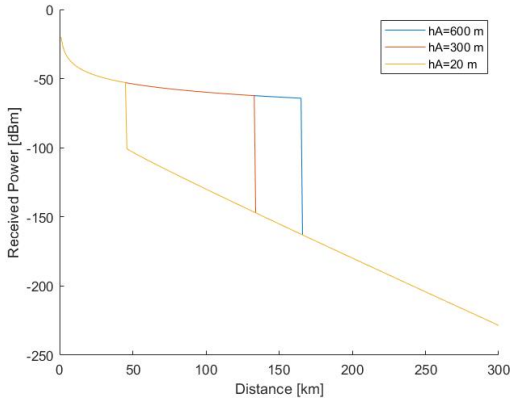

Figure 5. The power received as a function of the distance between terminals.

As a direct consequence, it was necessary to determine whether obstacles were being taken into account in the calculation of received power as a function of distance. The terrain profile corresponding to 240º was used for this, with the North Pole as a reference point, 0º. The expected outcome was three curves similar to Figure 5, but with some misalignment. These inconsistencies are caused by losses incurred by obstacles in the link's path. The obtained results confirmed the expectation and validated the existence of the three curves, which were partially overlapped and uneven due to the presence of obstacles that obstructed the connection.

All of the tests presented were carried out without regard for the radiation diagrams of the antennas used. As a result, it was necessary to determine whether the radiation diagrams would be properly considered in the calculations.

For this, tests were performed in which the evolution of the received power as a function of distance was compared in two different scenarios: the first in which the maximum gain value is considered, and the second in which the gain is dependent on the radiation diagrams. Both curves are expected to behave in a similar manner. However, for the same distance value, the curve that considers maximum gain has slightly higher received power values than the other curve.

Figure 6 shows that the developed model exhibits the expected behavior. As a result of all of the tests, it was determined that the model is appropriate for the analysis of the system to be implemented.

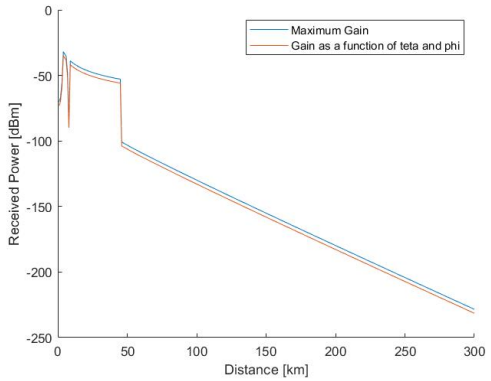

Figure 6. Power received as a function of terminal distance with obstacle attenuation.

IV. Results Analysis

A. Definition of Scenarios

Three aspects will be considered for the study: the location of the ground stations, the antennas installed in the aircraft, and the antennas that may be installed in the ground stations.

As a result, as previously stated, five distinct terrestrial stations will be considered, with locations in Flores, Faial, Terceira, São Miguel, and Santa Maria.

The expressions that describe the radiation diagrams of the terminal antennas were previously presented. The antennas of ground stations as well as the antennas installed on aircraft. This is important for carrying out the communications system project because it is necessary to understand which type of antenna is best suited for use in ground stations.

In this way, the research of several antennas compatible with the system's operational requirements was carried out.

To conduct the tests, two omnidirectional antennas were chosen from among the analyzed antennas: the one with the highest gain value and the one with the lowest gain value. A directional antenna with the highest gain was also chosen.

Omnidirectional antennas will be analyzed in two contexts: first, with the antenna on top of the support tower, and second, with the antenna at about two-thirds of the maximum height of the support tower. The fact that the omnidirectional antenna is not located on top of the support tower, as seen in the previous chapter, causes its radiation diagram to change, influencing the results of the coverage diagrams. In the second test, the antenna will be manipulated so that its maximum gain is directed to locations most affected by the shadow area, while keeping the same height in mind.

The radiation diagram for sectorial antennas will not change due to the support tower, so the location in terms of height in the same will not be a limiting factor in terms of the radiation diagram. However, the number of antennas used per terrestrial station will be evaluated in order to achieve total coverage provided by the set of antennas that is as close to an omnidirectional antenna as possible.

The first antenna under consideration is the 7500143 antenna, which is omnidirectional and has the lowest gain value of all those investigated. Table 4 lists the antenna features that are essential for the tests. Expressions (10) and (11) describe the vertical and horizontal radiation diagrams of the current antenna, respectively.

Table 4. Antenna Specifications 7500143.

Radiation Diagram	Omnidirectional
Gain [dBi]	2.2

The 470.31.05.00 antenna, which is also omnidirectional, was the second antenna studied. The antenna characteristics relevant for the tests are shown in Table 5. Expressions (12) and (11) describe the vertical and horizontal radiation diagrams of the current antenna, respectively.

Table 5.Antenna Specifications 470.31.05.00.

Radiation Diagram	Omnidirectional
Gain [dBi]	5.2

The horizontal radiation diagrams of the two antennas mentioned above are replaced by expression (13) in the second test, with the antennas at two-thirds of the maximum height of the support tower.

The third antenna under consideration is the S.M2-145 antenna, which will be the only sectorial antenna used in the tests. The antenna properties that will be relevant for the tests are shown in Table 6. Expressions (14) and (15) describe the vertical and horizontal radiation diagrams of the current antenna, respectively.

Table 6. Antenna Specifications S.M2-145.

Radiation Diagram	Sectorial
Half Power Beam Width	36º
Gain [dBi]	7.2

B. Omnidirectional Stations

The simplest configuration of the system was considered in the initial tests. That is, all ground stations are treated the same and have omnidirectional antennas. For this, tests were conducted using the two omnidirectional antennas located on top of the support towers at three different aircraft flight altitudes.

In the initial tests, the omnidirectional antenna 7500143 was used. When the results in Table 7 were analyzed, it was discovered that the current antenna does not meet the operating requirements, because the coverage range is much less than the required 200 km at an aircraft flight altitude of 600 m.

Table 7. Maximum coverage range when using antenna 7500143.

Maximum coverage range [km]		
Ground Stations	$h_A[m]$	
	20	**300 and 600**
Morro Alto	64	64
Cabeço Gordo	64	64
St. Bárbara	64	64
Barrosa	64	64
Pico Alto	46	64

The graphs of received power as a function of distance also revealed that there were many shadow zones in the vicinity of the terrestrial terminal, as shown in Figure 7.

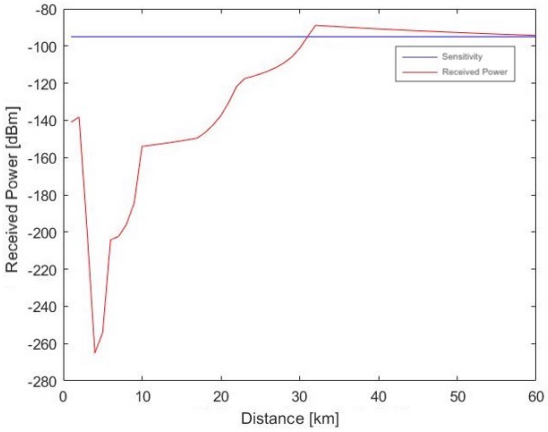

Figure 7. Power received as a function of distance in Morro Alto in the direction of 310º.

The omnidirectional antenna 470.31.05.00 was then tested to determine its performance.

Table 8 and Figure 8 show that when the antenna is mounted on top of the support tower, its performance meets the operational requirements. It was also determined that as the aircraft's flight altitude increased, the areas of the ground stations' shadow zones improved.

Table 8. Maximum coverage range when using antenna 470.31.05.00..

Maximum coverage range [km]			
Ground Stations	$h_A[m]$		
	20	**300**	**600**
Morro Alto	75	170	203
Cabeço Gordo	84	180	213
St. Bárbara	78	174	206
Barrosa	75	170	203
Pico Alto	46	134	166

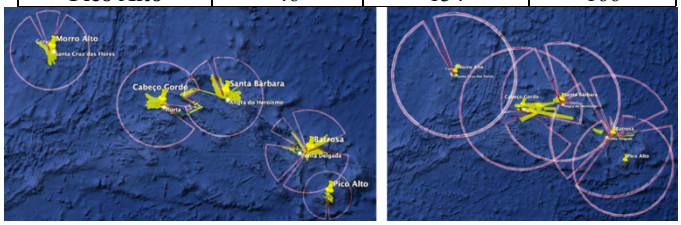

(a) 20 m Flight Altitude *(b) 600 m Flight Altitude*

Figure 8. Coverage and shadow diagrams of the 470.31.05.00 antenna on top of the support tower.

The antennas were considered on top of the support towers in all of the results presented in this section. The antennas were considered to be at a height of approximately two-thirds of the maximum height of the support tower in the following tests, as the antennas will be installed in towers where other equipment is already located, and thus the ideal location may not be possible. The various tests were carried out with the variables in mind, with the antennas directed to different locations, the three flight altitudes, and the two antennas. The results shown below are the best that could be obtained for the conditions under consideration.

When viewed from two-thirds of the maximum height of the support tower, the maximum range of both analyzed antennas remained unchanged. However, as shown in Figure 9 the coverage area has shrunk significantly.

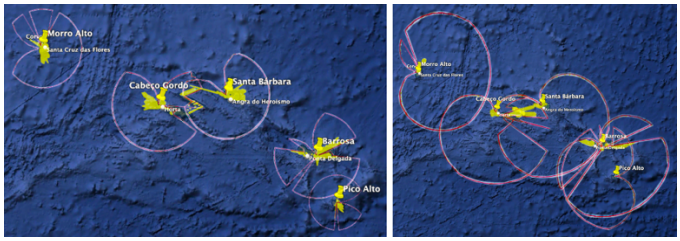

(a) 20 m Flight Altitude *(b) 600 m Flight Altitude*

Figure 9. Antenna coverage and shadow diagrams 470.31.05.00 at two-thirds of the top of the support tower.

When comparing the performance of the two antennas, it is clear that when placed at two-thirds of the maximum height of the support tower, both lose performance. It was also possible to confirm that, if an omnidirectional antenna is to be used in the system, the 470.31.05.00 antenna should be chosen because it is the only one of the two that meets the operational requirements and has lower shadow areas.

When considering the antenna 470.31.05.00, the figures show that the area between the ground stations of Cabeço Gordo and Santa Bárbara has the highest prevalence of the shadow zone. These shadow areas are caused by Pico Mountain, which generates losses due to obstacles, resulting in the connection being obstructed. Consequently, it was regarded as a ground station at the top of the Pico Mountain for research purposes. The antenna 470.31.05.00 was considered, placed in a 20-meter-high support tower, and knowing that the altitude of the point where the antenna is installed is 2,351 meters above sea level.

When the results were analyzed, it was discovered that the maximum range of this ground station was greater than the other ground stations, as expected, and the shadow zones were less extensive, as shown in Table 9 and Figure 10.

Table 9. Maximum coverage range when considering an alternative ground station on Pico Island using antenna 470.31.05.00

h_A[m]		20	300	600
Ground Station	**Pico**	145	242	275

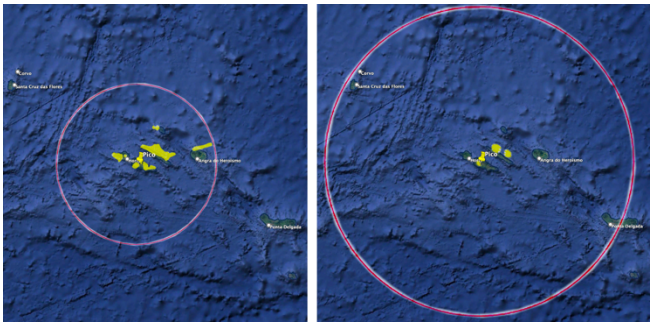

(a) 20 m Flight Altitude *(b) 600 m Flight Altitude*

Figure 10. Coverage and shadow diagrams of the 470.31.05.00 antenna on top of the support tower when considered a ground station on Pico Island

The maximum reach obtained in the majority of the cases studied was equal to the maximum distance of application of the free space model. This is due to the fact that the over-horizon model's loss value is much higher than the free space model's. As a result, the received power decreases significantly in the transition zone between the models, rendering communication impossible.

The linkage analysis did not take linkage quality assessment criteria into account. This is due to a continuous and regular decline in the quality of the connection until, in the transition zone between the models, there is an abrupt break and the connection between the terminals is no longer possible.

C. Sectorial Stations

The system's performance was then evaluated in light of the sectorial antenna. Their performance was tested for all ground stations and the three flight altitudes considered in the study, just like omnidirectional antennas. Two antenna configurations were tested: the first with two sectorial antennas per terrestrial station and the second with three sectorial antennas. The goal would be to obtain a coverage diagram that resembles that of an omnidirectional antenna. As a result, it was determined that three S.M2-145 type antennas would be required to provide the desired coverage.

As a result, Table 10 shows the system's maximum range values for the three aircraft flight altitudes when the antennas are considered at the top of the support tower with a 120º difference between them. The maximum coverage range diagrams and shadow diagrams for the Cabeço Gordo ground station are shown in Figure 11. These diagrams depict a scenario in which the aircraft is at a height of 600 meters and the antennas are considered at the top of the support tower, with the omnidirectional antenna 470.31.05.00 and the set of sectorial antennas S.M2-145.

When comparing Tables 8 and 10, it was discovered that the configuration with the omnidirectional antenna 470.31.05.00 or with the set of sectorial would have very similar maximum coverage ranges. The Pico Alto land station in Santa Maria saw only a minor increase. In absolute terms, there was a 1 km increase, and in relative terms, there was a 2.2 % increase. The differences, however, are related to the shadow areas obtained. As shown in Figure 11, the shadow zones of the Cabeço Gordo ground station when using the set of three sectorial antennas S.M2-145 are significantly smaller than the shadow zones obtained with the omnidirectional antenna 470.31.05.00.

Table 10. Maximum coverage range when using the set of three S.M2-145 antennas

Maximum coverage range [km]			
Ground Stations	$h_A[m]$		
	20	**300**	**600**
Morro Alto	75	170	203
Cabeço Gordo	84	180	213
St. Bárbara	78	174	206
Barrosa	75	170	203
Pico Alto	47	135	167

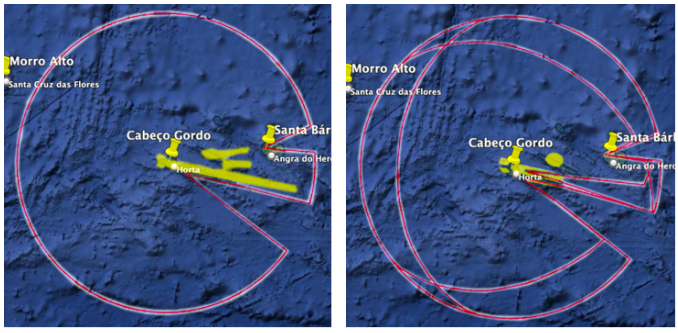

(a) 470.31.05.00 Antenna *(b) S.M2-145 Antenna*

Figure 11. Coverage range and shadow areas of the Morro Alto ground station

This pattern was observed for all ground stations, with the shadow zones significantly reduced when the set of three sectorial antennas was used.

Following that, the performance of this same configuration was examined when the antennas were installed at two-thirds of the support tower's maximum height. When analyzing the obtained results, it was discovered that the difference in heights between the two antenna configurations is insufficient to have a significant influence on the obtained results. As a result, in terms of the maximum coverage range, the values in Table 10 can be used as a reference for the maximum ranges obtained. When it came to the shadow areas, they remained unaltered.

When the performance of the two antennas is compared, it is concluded that, if the antenna is installed on top of the support tower, both the omnidirectional antenna 470.31.05.00 and the set of three sectorial antennas S.M2-145 meet operational requirements. However, because it is also intended to reduce shadow areas as much as possible, the best configuration for the system, if the antennas can be installed on top of the support tower, would be to use a set of three sectorial antennas. Because it does not meet operational requirements, omnidirectional antenna 7500143 has been excluded.

When the antennas have to be placed at two-thirds of the maximum height of the support tower, the choice is between the omnidirectional antenna 470.31.05.00 and the three sectorial antennas S.M2-145. When the performance of the antennas is evaluated, it is determined that the best configuration would be a set of three sectorial antennas.

As a result, while the omnidirectional antenna 470.31.05.00 meets the operational requirements, the use of three sectorial

antennas S.M2-145 is the best alternative to apply to the system, regardless of the height at which the antennas are installed.

V. Conclusions

The goal of this dissertation was to create a model that would optimize the coverage of the aeronautical communications system that would be installed in the Azores while taking operational requirements into account. The goal of this optimization was to increase the maximum coverage range while decreasing shadow areas as much as possible. As a result, a similar system that was once installed in the Azores archipelago was considered in an early phase of the analysis of possible future system characteristics. The system under consideration is intended to aid in search and rescue missions.

During the model's development, the generic view of the model that will be implemented is presented, as well as the model application scenarios and all system characteristics required to implement the model. As a result, three different scenarios were considered. All scenarios assume that the results obtained must meet the operating requirements, i.e. that at a maximum altitude of 600 m, a coverage range of at least 200 km is achievable. The three scenarios consider the flight altitudes of the two aircraft that typically carry out this type of mission, so three different flight altitudes will be studied: 20, 300, and 600 m.

The power received at the terminals was analysed to determine whether there was coverage along the radial path in relation to the ground stations. In the initial tests, the characteristics of the system that was previously installed in the Azores were used. Thus, the gain of the ground stations was 2.5 dBi, the operating frequency was 139.3 MHz, the terminal sensitivity was -95 dBm, and the emission power was 43 dBm. It was also thought to have a gain of aircraft antennas of -3 dBi.

Following that, a study of the propagation models that have application in the system under study is carried out, with the conclusion that the free space propagation model, the trans-horizon communication model, and the Knife-edge and Deygout's model will be used for the model. The remaining models were eliminated because their maximum application distances were less than the models' minimum application distances.

Fading can have an impact on communication performance. The fading that will have the greatest impact in the case under consideration will be the fast fading. The worst-case scenario was considered during the model's development, and thus the fading margin considered typical for moving terminals was used. As a result, a fading margin of 15 dB was considered.

Additionally, radiation diagrams of the various antenna possibilities to be installed in the system, as well as the radiation diagrams of aircraft antennas, are presented.

Finally, a measurement of the developed model is performed, noting whether the models exhibit the expected behaviour when compared to theoretical results, as well as comparing the evolution of the developed model's results with the expectation. At the conclusion of this evaluation, it was determined that all results were in accordance with expectations, and thus the model could be applied to the system under study.

Finally, in the first phase of the results analysis, the scenarios for applying the model are presented. The results of the model's benchmarking are taken into account in the evaluation of the scenarios. Different types of antennas are also considered in the scenarios, two of which are omnidirectional and one of which is sectorial.

As a result, various antennas and their radiation diagrams were evaluated. Because the installation of antennas in the support tower may be dependent on other antennas previously installed, two different scenarios for antenna placement were considered. The first scenario involved thinking about the antennas installed on top of the support towers. The antennas at two-thirds of the maximum height of the support tower were considered in the second scenario.

The installation of three sectorial antennas per terrestrial station was considered. As a result, the sum of the radiation diagrams of the three antennas equals the radius of an omnidirectional antenna's radiation diagram.

As previously stated, three distinct antennas were considered. Two of them are omnidirectional, one with a maximum gain of 2.2 dBi, the 7500143 antenna, and another with a maximum gain of 5.2 dBi, the antenna 470.31.05.00, as well as a sector antenna, the S.M2-145 antenna, with a maximum gain of 7.2 dBi. The goal would be to understand the performance differences between the antennas under consideration and determine whether they met the operational requirements. Following that, it was intended to determine whether there were any significant improvements when comparing the results of these antennas to the sectorial antenna. The results were compared based on the coverage range as well as the area of the existing shadow zones.

Several tests were performed with the investigated antennas in order to determine the best configuration for the system under consideration, and the possibility of existing alternative locations for ground stations to improve performance was also investigated.

As a result, we began by examining the system's most basic configuration, in which the same omnidirectional antennas were considered in all ground stations and on top of all ground stations' support towers. When the results of the 7500143 antenna were examined, it was discovered that it did not meet the operational requirements.

When the results of the antenna 470.31.05.00 were examined, it was discovered that this antenna met the operational requirements for the ground stations of Morro Alto, Cabeço Gordo, Santa Bárbara, and Barrosa, with the lowest maximum range value being 203 km. Because the Pico Alto ground station has a maximum range of 166 km, it cannot meet the operational requirements. The antennas were discovered to be approximately two-thirds of the maximum height of the support tower in the following tests. When comparing the performance of the two antennas, it is clear that when placed at two-thirds of the maximum height of the support tower, both lose performance. It was also possible to see that, if you choose to use an omnidirectional antenna in the system, the 470.31.05.00 antenna is the only one that meets the operational requirements and has lower shadow areas.

When considering the antenna 470.31.05.00, it was also discovered that the area between the ground stations of Cabeço Gordo and Santa Bárbara has the highest prevalence of shadow areas. The Pico Mountain, which is located between the islands of Faial and Terceira, is responsible for these shaded areas. As a result, a ground station at the summit of Pico Mountain was considered for research purposes.

When analysing the results obtained, it was observed that, if there was the possibility of installing a land station on top of Pico Mountain, its maximum range would be greater than that of the

other land stations, reaching a value of 275 km, and the areas of shadows were less extensive, another advantage is the fact that the coverage provided by this ground station has the ability to mitigate most of the shadow zones of the ground stations around it.

Following that, the system's performance was evaluated in light of the sectorial antenna. Their performance was tested for the five ground stations and the three flight altitudes considered in the study, just like the omnidirectional antennas. When the system was configured with sectorial antennas, it was discovered that three S.M2-145 type antennas would be required to provide the desired coverage.

When the performance of the omnidirectional antenna 470.31.05.00 was compared to the set of three sectorial antennas S.M2-145, the maximum range of the two antennas was found to be equal. The shadow areas, on the other hand, showed significant differences, and their area decreased when the three sectorial antennas were used. It was also discovered that the Cabeço Gordo ground station had the most significant improvements.

Following that, the performance of this same configuration was examined when the sectorial antennas were installed at two-thirds of the support tower's maximum height. When the obtained results were analysed, it was discovered that the difference in heights between the two antenna configurations was insufficient to influence the obtained results, leaving the maximum range and shadow zones unchanged.

When the performance of the three antennas is compared, it is determined that antenna 7500143 is out of the running because it does not meet the operational requirements. It was also determined that if the antenna could be installed on top of the support tower, both the omnidirectional antenna 470.31.05.00 and the three sectorial antennas S.M2-145 would meet the operational requirements. However, because the goal is to minimize shadow areas as much as possible, the best system configuration would be to use a set of three sectorial antennas.

In the study, all terrestrial stations considered were at the highest point on the respective island, implying that there are no alternative locations that improve system performance when compared to the locations considered. However, when the possibility of installing an earth station on Pico Island was investigated, it was discovered that this would be an alternative location that would bring system improvements, as its reach would lead to certain shadow areas being mitigated and, also, because the shadow zones of this earth station are reduced. This alternative, however, is unlikely to materialize due to the impossibility of installing the antennas in this location, as there is no infrastructure required for this purpose in this location. Another reason for the ground station's impossibility is logistical issues, such as difficult access to the location under consideration.

The results of the tests revealed that the maximum coverage range was equal to the transition distance between the free space and trans-horizon models in many of the cases studied. This is due to the fact that the value of path losses increases significantly when switching between the two models.

The quality of service was not evaluated in depth because the quality of the connection gradually and continuously degrades with distance until, at the point of transition between propagation models, the connection is completely degraded.

REFERENCES

[1] Assembleia da República, Parlamento-Estatuto e Competências-Constituição da República Portuguesa-Artigo 275º, 2005. (https://www.parlamento.pt/Legislacao/Paginas/ConstituicaoRepublicaPortuguesa.aspx).

[2] Estado Maior da Força Aérea, Missão – Visão, 2020. (https://www.emfa.pt/p-181-missao_visao).

[3] Estado Maior da Força Aérea, Base Aérea nº4 – História, 2020. (https://www.emfa.pt/unidade-27-base-aerea-n-4).K. Elissa, "Title of paper if known," unpublished.

[4] Estado Maior da Força Aérea, Esquadra 502 – Destacamento Aéreo dos Açores, 2020. (https://esquadra.emfa.pt/link-502-005.003.002-daa).

[5] Estado Maior da Força Aérea, Esquadra 751, 2020. (https://www.emfa.pt/esquadra-46-esquadra-751-pumas).

[6] FAP Oficial – *Instagram,* 2020. (https://www.instagram.com/p/CJnZagilVa0/?utm_source=ig_web_copy_link).

[7] Cartil – Telecomunicações e Eletrónica, S.A., Telas Finais Sistema de Comunicações VHF para o Arquipélago dos Açores, Lisboa, Portugal, 2008.

[8] Estado Maior da Força Aérea, Relatório Confidencial – Sistema de Comunicações VHF Militar sediado nos Açores, 2020.

[9] Bower A., Chandler D., "*Extended Range VHF Communications improve performance of air transport operations"*, *ICAO Journal*, Vol.57, Nº3, pp.23 e pp.31, Nov. 2002.

[10] Park Air Systems – *A Northrop Grumman Companny*, https://www.parkairsystems.com/components/t6-vhf-uhf-radio, Jan 2021.

[11] Marsh, G., *Longer Legs for VHF, Avionics Magazine,* Mar. 2004. (http://www.aviationtoday.com/av/air-traffic-control/Longer-Legs-for-VHF_780.html)

[12] ICAO, VHF coverage over Indian Airspace, Eight Meeting of the Communications/Navigation/Surveillance and Meteorology Sub-Group (CNS/MET SG/8) of APANPIRG, Thailand, July 2004. (http://www.icao.int/Meetings/AMC/MA/2004/CNSMET_SG(/ip20.pdf).

[13] Estado Maior da Força Aérea, Relatório Confidencial – Sistema de Comunicações VHF Militar sediado nos Açores, Lisboa, Portugal, 2020.

[14] Pereira, A., Operacionalização, no contexto da Força Aérea, de um Sistema Aéreo Autónomo Não-Tripulado Classe II para Vigilância Marítima e Busca e Salvamento, Tese de Mestrado, Academia da Força Aérea, Sintra, Portugal, 2016 (https://comum.rcaap.pt/bitstream/10400.26/14369/1/DISSERTACAO_ASPAL_PILAV_PEREIRA.pdf).

[15] ITU, *Reflection from the surface of the Earth, ITU-R Report 1008-1, Switzerland*, 2021

[16] Rodrigues, A., Sanguino, J., Feixes Hertzianos – Formulário, Material de Apoio à Unidade Curricular de Sistemas de Telecomunicações Via Rádio, Instituto Superior Técnico, Lisboa, Portugal, 2020 (https://fenix.tecnico.ulisboa.pt/disciplinas/STVR77/2020-2021/1-semestre/material-de-apoio).

[17] ITU, Propagation by diffraction, ITU-R Recommendation P.526-14, Switzerland, 2018.

[18] Sadeque, Md., Mohonta, S., Ali, Md., *Modeling and Characterization of Different Types of Fading Channel*, International Journal of Science, IJSETR, Vol.4, May 2015. (https://www.researchgate.net/profile/Md-Golam-Sadeque/publication/336579078_Modeling_and_Characterization_of_Different_Types_of_Fading_Channel/links/5da6dc28299bf1c1e4c3a501/Modeling-and-Characterization-of-Different-Types-of-Fading-Channel.pdf).

[19] Hoeher, P., Haas, E., Aeronautical Channel Modeling at VHF-Band, Information and Coding Lab, University of Kiel, Institute for Communication Technology, German Aerospace Center, Germany, 2021 (https://ieeexplore.ieee.org/document/797280